

Microelectromechanical Systems (MEMS) Accelerometers Using Lead Zirconate Titanate Thick Films

L.-P. Wang, K. Deng, L. Zou, R. Wolf, R. J. Davis, and S. Trolier-McKinstry

Abstract—MEMS accelerometers based on piezoelectric lead zirconate titanate (PZT) thick films with annular diaphragm sensing structures were designed, fabricated, and tested. Theoretical and numerical models for this new inertial sensing structure are presented. The design provides good sensitivity along one axis, with low transverse sensitivity and good temperature stability. Test results show high sensitivities and broad usable frequency ranges. Measured sensitivities range from 0.77 to 7.6 pC/g for resonant frequencies from 35.3 kHz to 3.7 kHz. Reasonable agreement with theoretical values was obtained.

Index Terms—Microelectromechanical devices, micromachining, piezoelectric films, sensors.

I. INTRODUCTION

IN 1998, accelerometers based on microelectromechanical systems (MEMS) enjoyed the second largest yearly sales volume, after pressure sensors, of all MEMS devices [1]. While reviews of capacitive and piezoresistive accelerometers are given elsewhere [1]–[3], less literature is available on piezoelectric MEMS accelerometers. In the latter, ZnO and PZT films are the two primary sensing materials used. For sensor applications, PZT is suitable for operating in charge mode since its dielectric constant is much higher comparing to ZnO [4]. Typically, the charge sensitivities of MEMS accelerometers using ZnO films are relatively small [5]–[8] since the electromechanical coupling coefficients and the piezoelectric constants of ZnO are an order of magnitude smaller than those of PZT films.

Kim *et al.* [9] fabricated surface-micromachined PZT accelerometers with a cantilever-beam structure. No dynamic frequency response measurements were given. Bulk-micromachined PZT accelerometers using a seismic mass and two silicon beams as the sensing structure were fabricated by Eichner *et al.* [10]. An average sensitivity of 0.1 mV/g was measured, and the calculated resonant frequency was 13 kHz. Beeby *et al.* [11], [12] fabricated a bulk micromachined accelerometer using screen-printed PZT thick films. The

Manuscript received December 3, 2001; revised January 18, 2002. This work was supported by the National Institute of Standards and Technology under WR-ATP-0001, the Penn State Nanofabrication Facility, and the Cornell Nanofabrication Facility, which provided the DRIE tool. The review of this letter was arranged by Editor J. Sin.

L.-P. Wang, R. Wolf, R. J. Davis, and S. Trolier-McKinstry are with Pennsylvania State University, University Park, PA 16802 USA.

K. Deng and L. Zou are with Wilcoxon Research, Gaithersburg, MD 20878 USA.

Publisher Item Identifier S 0741-3106(02)03208-1.

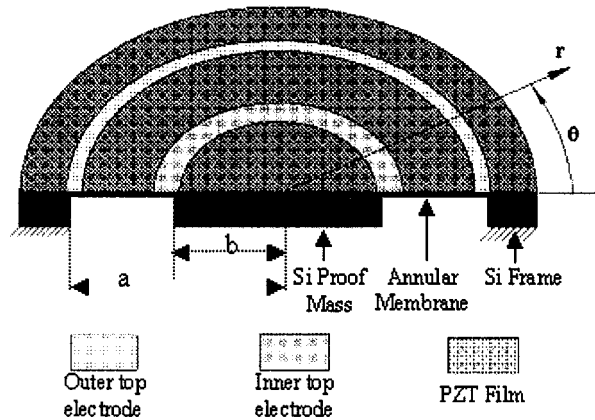


Fig. 1. Schematic showing the cross section of an annular diaphragm MEMS accelerometer.

reported sensitivity of 16 pC/g seems somewhat high, however, since the acceleration-induced stress integrated over the area of the piezoelectric should be lowered since the stresses are of opposite sign near the frame and the inertial mass. In addition, the reported voltage sensitivity, 100 μ V/g, is inconsistent with the charge sensitivity for the sensor capacitance of 360 pF.

This letter reports the successful fabrication and testing of piezoelectric accelerometers based on thick film PZT and deep-trench reactive ion etching (DRIE).

II. DEVICE DESIGN AND FABRICATION

This paper describes a circular diaphragm sensing structure [13], specifically, an annular membrane supported by a silicon frame with a proof mass suspended at the center of the diaphragm (See Fig. 1). The thickness of the Si layer supporting the PZT film/electrode stack is between 6 and 45 μ m. The piezoelectric film is deposited on a Pt/Ti/SiO₂ stack so that it can be poled through its thickness and the annular top electrodes are adjusted so that the areas are identical. The pyroelectric effect is cancelled when these two area are poled in the opposite directions. Compared with beam-type sensing structures, this design uses area efficiently, yielding a high sensitivity accelerometer. Because the structure is stiff, the sensor has a high resonant frequency and wide bandwidth. Furthermore, the symmetry yields natural insensitivity to transverse acceleration. From a fabrication standpoint the design does not require through-etching the silicon to release the membrane, therefore, the fabrication process is simplified and yield can be enhanced.

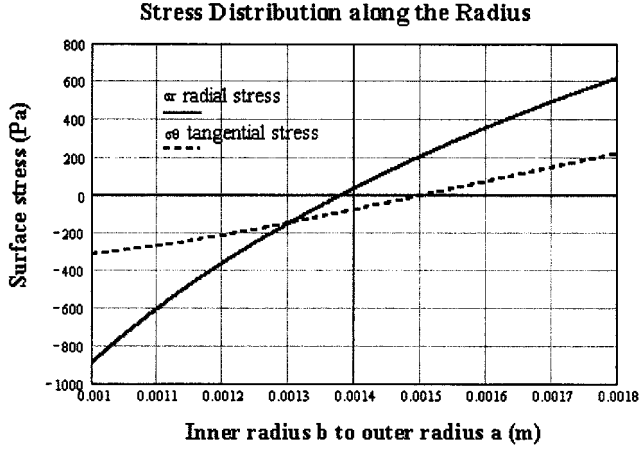


Fig. 2. Modeled stress distribution in the accelerometer along the radial direction; the solid line is radial stress, and the dashed line is tangential stress.

The structure was modeled using Timoshenko plate theory [14], and the boundary conditions under quasistatic inertial load were treated as in [15]. The analytical stress solutions are

$$\text{Radial stress: } \sigma_r = \frac{M}{4\pi D} \cdot \left(\frac{h}{2} \frac{d^2 w}{dr^2} + \frac{h v_f}{2 r} \frac{dw}{dr} \right)$$

$$\text{Tangential stress: } \sigma_\theta = \frac{M}{4\pi D} \cdot \left(\frac{h}{2r} \frac{dw}{dr} + \frac{h}{2} v_f \frac{d^2 w}{dr^2} \right)$$

where M is the cylindrical mass, D is the flexural stiffness of the plate, v_f is the PZT film Poisson's ratio, h is the membrane thickness, and w is the membrane deflection function.

In this structure, both radial stresses and tangential stresses contribute to the piezoelectric charge (see Fig. 2). However, the stresses are of opposite signs for the outer (i.e., close to the frame) and inner sides of the diaphragm; therefore, the top electrodes are separated in order to pole the two sections in opposite directions. When the outputs of the electrodes are connected in parallel, the pyroelectric output of the sensor is cancelled. To lower the overall sensor capacitance (to ~ 6 nF), the top electrodes are placed only over highly stressed areas. The overall sensor size was 6 mm \times 6 mm.

The fundamental resonance frequency of this structure was derived by the Rayleigh energy method [16]

$$\omega_0 = 2\sqrt{\pi} \cdot \frac{\sqrt{C(\lambda)}}{b} \sqrt{\frac{D}{M}}$$

where b is the inner radius, λ is the ratio of the outer radius to the inner radius, and $C(\lambda)$ is

$$C(\lambda) = \frac{4(\lambda^2 - 1)}{[(\lambda^2 - 1)^2 - (2\lambda \cdot \ln \lambda)^2]}$$

Using this function, the resonant frequency and the charge sensitivity were $\leq 8\%$ different from the numbers calculated by finite element analysis, for inner and outer radii of ~ 1 mm and 2 mm respectively. A higher resonance frequency will provide a larger usable frequency range, at the expense of reduced sensitivity.

The MEMS accelerometers reported here (see Fig. 3) were fabricated using 5.6 μm -thick chemical-solution-derived PZT

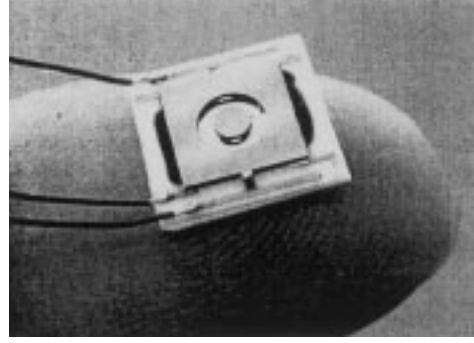


Fig. 3. View of the backside of an annular MEMS accelerometer. The front side is flip-chip bonded with a ceramic substrate.

films and DRIE bulk-micromachining techniques. Multiple deposition and crystallization steps were used to build up the PZT thickness. The fabrication processes will be detailed in [17].

III. MEASUREMENTS

Dynamic frequency response measurements were performed to evaluate the accelerometers. The devices were attached to ceramic substrates with screen-printed contact pads and then the contact pads of the sensors on the frame area were wire-bonded to them. Wires were soldered to the ceramic substrates for signal output. The MEMS accelerometer was connected to a charge amplifier with an amplification of 10 mV/pC. The reference accelerometer (Wilcoxon Research 05 238) was connected to a charge amplifier (Wilcoxon Research CC701). The outputs of both accelerometers were connected to a two-channel dynamic signal analyzer for a comparative transfer function measurement. A swept-sine signal, generated by the analyzer and enhanced by a power amplifier, was used to drive an electromagnetic shaker (Wilcoxon Research AV50) to mechanically excite both accelerometers. Fig. 4 shows the measured frequency response of one fabricated MEMS accelerometer.

IV. RESULTS AND DISCUSSION

Good sensitivities and broad usable frequency ranges (see Table I) were obtained. The sensitivities range from 0.77 to 7.6 pC/g with resonant frequencies from 35.3 to 3.7 kHz. The sensor-to-sensor variations were caused largely by variations of the silicon membrane thickness because of nonuniformity in the Si DRIE etching. The measured sensitivities were -2 to 30% different from sensitivity calculated from finite element analysis using a value for the $d_{31(\text{eff})} \times$ Young's modulus for the PZT film of -4.5 C/m², which was measured on a test die on the same wafer [17]. The accuracy of the $d_{31(\text{eff})} \times$ Young's modulus is $\pm 7\%$ [18]. The transverse sensitivity was found to be $< 2\%$ of the sensitivity along the principal axis.

The discrepancy between the measured sensitivity and the FEA calculations is believed to be due to the ~ 20 μm tolerance in the mechanical front and backside alignment, residual stress in the membrane, and piezoelectric film variations. Further improvement in fabrication consistency and noise floor measurement are expected in future runs. Additional modeling will facilitate optimization of the MEMS sensor design.

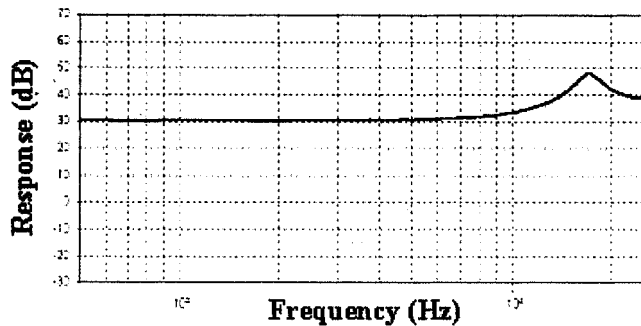


Fig. 4. Typical frequency response of a MEMS accelerometer reported here. The resonant frequency is 17.4 kHz and the subresonance sensitivity is 1.4 pC/g. The curve shows a typical frequency response of a MEMS prototype accelerometer from 500 Hz to 25 kHz. For frequencies lower than 500 Hz, a flat frequency response range (~ 60 to 500 Hz) can be obtained with appropriate electronics.

TABLE I
MEASURED RESULTS IN COMPARISON TO THE SIMULATED RESULTS

Chip No.	Measured Results		FEA Calculation	
	Resonant Frequency (kHz)	Sensitivity (pC/g)	Sensitivity ^{1,2} (pC/g)	Silicon membrane thickness ¹ (μm)
1	3.7	7.60	7.45	6.1
2	17.4	1.45	2.10	21.2
3	27.5	1.06	1.18	36.8
4	35.3	0.77	0.84	44.4

Note:

- The thickness of the Si diaphragm was calculated based on the measured resonance frequency. The FEA sensitivity was then recalculated based on this Si thickness. The thickness of PZT film is $5.6\mu\text{m} \pm 0.09\mu\text{m}$ for all devices.
- The product of $d_{31(\text{eff})}$ * Young's modulus for the PZT film used in the calculation was -4.5 C/m^2 .

V. CONCLUSIONS

Piezoelectric MEMS accelerometers using an annular diaphragm and $5.6 \mu\text{m}$ thick PZT films demonstrate high

sensitivities (0.77 to 7.6 pC/g) and broad usable frequency ranges (35.3 to 3.7 kHz). The annular piezoelectric inertial sensing structure is an efficient design and is compatible with the piezoelectric film and IC fabrication processes.

REFERENCES

- [1] N. Yazdi, F. Ayazi, and K. Najafi, "Micromachined inertial sensors," *Proc. IEEE*, vol. 86, pp. 1640–1659, Aug. 1998.
- [2] C. Song, B. Ha, and S. Lee, "Micromachined inertial sensors," in *Proc. 1999 IEEE/RSJ, Int. Conf. Intelligent Robots and Systems*, vol. 2, 1999, pp. 1049–1056.
- [3] S. M. Sze, *Semiconductor Sensors*. New York: Wiley, 1994.
- [4] P. Muralt, "Ferroelectric thin films for micro-sensors and actuators: A review," *J. Micromech. Microeng.*, vol. 10, pp. 136–146, 2000.
- [5] P. L. Chen, R. S. Muller, R. D. Jolly, G. L. Halac, R. D. White, A. P. Andrews, T. C. Lim, and M. E. Motamedi, "Integrated silicon microbeam Pi-FET accelerometer," *IEEE Trans. Electron Devices*, vol. ED-29, pp. 27–33, Jan. 1982.
- [6] P. L. Chen and R. S. Muller, "Integrated silicon Pi-FET accelerometer with proof mass," *Sens. Actuators*, vol. 5, pp. 119–126, 1984.
- [7] D. L. DeVoe and A. P. Pisano, "A fully surface-micromachined piezoelectric accelerometer," in *IEEE Int. Conf. Solid-State Sensors and Actuators*, vol. 2, Chicago, IL, 1997, pp. 1205–1208.
- [8] R. de Reus, J. O. Gulløv, and P. R. Scheeper, "Fabrication and characterization of a piezoelectric accelerometer," *J. Micromech. Microeng.*, vol. 9, pp. 123–126, 1999.
- [9] J. H. Kim, L. Wang, S. M. Zurn, L. Li, Y. S. Yoon, and D. L. Polla, "Fabrication process of PZT piezoelectric cantilever unimorphs using surface micromachining," *Integr. Ferroelectr.*, vol. 15, pp. 325–332, 1997.
- [10] D. Eichner, M. Giousouf, and W. von Munch, "Measurements on micro-machined silicon accelerometers with piezoelectric sensor action," *Sens. Actuators A*, vol. 76, pp. 247–252, 1999.
- [11] S. P. Beeby, N. Ross, and N. M. White, "Thick film PZT/micromachined silicon accelerometer," *Electron. Lett.*, vol. 35, no. 23, pp. 2060–2062, 1999.
- [12] —, "Design and fabrication of a micromachined silicon accelerometer with thick-film PZT sensors," *J. Micromech. Microeng.*, vol. 10, pp. 322–328, 2000.
- [13] "PSU Invention Disclosure," U.S. Patent Pending no. 2001-2435.
- [14] S. Timoshenko and S. Woinowsky-Krieger, *Theory of Plates and Shells*, 2nd ed. New York: McGraw-Hill, 1959.
- [15] A. Leissa, *Vibration of Plates*. Washington, DC: Sci. Tech. Inform. Div., NASA, 1993.
- [16] A. A. Shabana, *Vibration of Discrete and Continuous Systems*, 2nd ed: Springer-Verlag New York, 1997, p. 245.
- [17] L.-P. Wang, "Microelectromechanical systems (MEMS) sensors based on lead zirconate titanate (PZT) films," Ph.D. dissertation, Pennsylvania State Univ., University Park, 2001.
- [18] J. F. Shepard, P. J. Moses, and S. Trolier-McKinstry, "The wafer flexure technique for the determination of the transverse piezoelectric coefficient (d_{31}) of PZT thin films," *Sens. Actuators A*, vol. 71, pp. 133–138, 1998.